

NUMERICAL ANALYSIS AND COMPARISON WITH RESULTS OF FRACTURE TESTS OF LUG MANUFACTURED IN COMPOSITE MATERIAL

G. C. Fonseca¹ & S.F.M. Almeida²

¹Embraer – Centro de Engenharia e Tecnologia, Minas Gerais, Brasil

²Instituto Tecnológico de Aeronáutica - ITA, São José dos Campos, Brasil

Abstract

The objective of this paper is the comparison of the fracture between the numerical results and tensile tests in the region where failure occurred in a high thickness lug made of composite material subjected to longitudinal loading. Some points were developed: the calculation methodology and models used to predict the fracture region and type of failure using a finite element methodology presenting the numerical results, as well as the methodology to perform the tests on the specimens and the region after the component failure. The result of this work will be the comparison between numerical results and the experimental results of the fracture of this component in the failure region. In addition micro-structural analysis will be done to evaluate possible damages resulting from the manufacturing process in the specimens before the test.

Keywords: thick laminate, material composite, finite element method, fracture analysis

1. Introduction

The prediction of behavior in a structure when submitted on work loads and the response of propagation cracks on the structure is a challenge of engineering structural in special for composite thick laminates. This work is intended to determine using finite element method modelling to analyse crack propagation on thick composite structure, manufactured by RTM method with optimum thickness under a specific application for loading conditions.

Studies have shown to be efficient when it is possible to correlate the properties of the material, numerical simulations and methodologies of crack propagation and component failures. Comparisons between numerical analyses and experimental results are extremely valuable when it comes to component failures for engineering applications. This development methodology can avoid the failure of the component in service avoiding major problems.

Numerical simulation using the finite element method is an important tool used in structural analysis, and its application is not restricted only to the project, but it is also used in the study of failures. This tool has already been used to analyse the failure occurred in an aircraft lug made from composite materials of high thickness. Were performed studies for values verification of structural element loads can be used to attached horizontal and vertical stabilizer type "T".

Structures made of composite materials, regardless of the method of manufacture, are susceptible to the occurrence of several types of imperfections endangering product integrity. These defects can occur due to the manufacturing process or even result of a damage in service.

Thus, the typical load found on literature is 80kN used in typical executive class aircraft. The attached element between stabilizers is responsible for transfer all loads on the structure getting subject several structural efforts. This value and loading are used for basis in all development of this work with parameter for numerical simulations. For simplification of loads on this study is adopt just static loading applied parallel on plane of piece.

NUMERICAL ANALYSIS AND FRACTURE TESTS OF COMPOSITE MATERIAL LUG

This study demonstrated the variation of mechanical properties according to different plies orientations of laminate. Therefore the most appropriate value of joint with hole manufacture by composite material can be determined for $90^{\circ}/0^{\circ}$ orientation, that presented higher value of resistance.

Ransom *et. al* [1], performed studies about accident occurred in 587 flight of American Airlines with the Airbus A300-605R aircraft. As described in the NTSB report on the accident, the vertical tail separation was the result of loads beyond the design ultimate load that were created by the excessive rudder pedal inputs. Was presented general analysis about the accident, included experimental and computational methodologies used during investigations. The investigations were divided in two groups. The first group treated global analysis of problem, and used global strain, load of transfer and failure modes of vertical tail and rudder, both manufactured by composite material. The second group performed local lug analysis and concentrate in laminated failure component manufactured by composite material, that responsible for attached between vertical tail and fuselage. Figure 1 shows the vertical tail of the aircraft as well as the results of the analysis of the initial failure site (i.e., the right rear lug, one of the six carbon/epoxy composite lugs that connected the vertical tail to the fuselage).

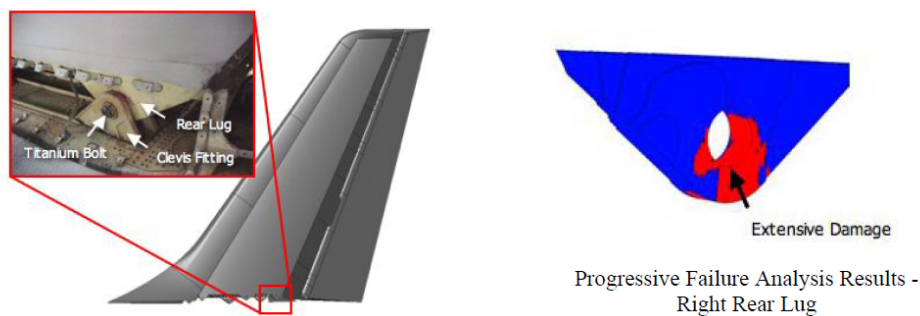


Figure 1 – Laminated composite lug failure on American Airlines, [1].

The laminated lug failure manufacture by composite material that result of accident with AirBus A300-605R is showed in Figure 2 .



Figure 2 – Accident of AirBus A300-605R with lug failure manufactured by composite material.

With this, it is necessary to know the behaviour of these components in service contributing significantly to the development of methodologies of failure analysis. The results of this work is analytical comparisons between physical and numerical results failure of thick lug manufacture by composite material.

2. Methodology

The studies are divided into parts:

1st. part) Preparation and analyse of samples micrography: In this part of the study the two types of samples are prepared and analysed. The first set relates to samples taken from a component before the test to evaluate fails on the manufacturing process with regard to voids and porosities. The second set of samples will be drawn from a component tested in the region where the catastrophic failure occurred during the test to analyse the fracture in that region. In this first part the criteria for withdrawal of the samples in the two components will be detailed, as well as the methods of preparation and analysis of the results.

2nd. part) Numerical simulations: Models were elaborated using finite element models on software Abaqus to obtaining numerical results. For this model will be mentioned the contact mechanism and the iterations used, further the formulation of the failure model, including the criterion and the evolution of the damage in the fibre and in the matrix and the procedure for degradation of material properties. The results obtained will be presented and discussed in next part.

3rd. part) Comparative analysis of experimental and numerical results: The results on the manufacturing process with regard to voids and porosities will also be presented in this part of the study. In this part are analyse and compared the numerical and experimental results of the failure region of the component in order to characterize the types of fractures in the component tested by validating the similarity.

All parts will be describe with more details in next subsections of this study.

3. Micrography analyses - manufacture and failure

Structures manufacture by composite materials, independently of manufacturing process are susceptible to the occurrence of many types of defects. Among of defects can be mentioned: voids and porosities, inclusions, region of accumulate resin, wrong plies alignment or orientation, creases in the superficial plies and debonding in case of laminates structures with core.

These defects can occur due to manufacturing process or even as a result of damage in service, according to Ancelloti Junior [3].

Figures 3 and 4 shows photomicrographs of composite carbon fibre with resin epoxi matrix and present a aleatory distribution of voids along the thickness of the analyzed material.

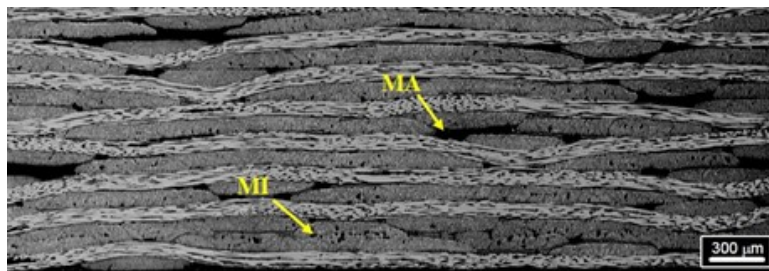


Figure 3 – Photomicrographs section of analysed material, [3].

Where is indicated on Figure 3 MI - micro voids, represents size between 7 to 30 μm , and where is indicated MA, means macro voids with average size between 30 to 600 μm .

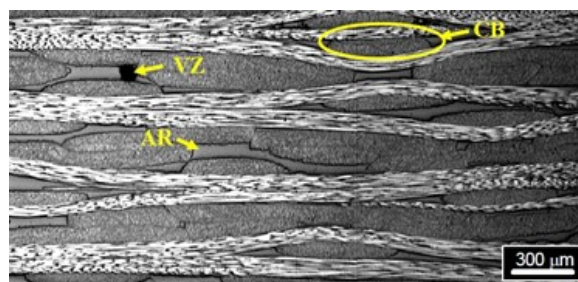


Figure 4 – Photomicrographs section of analysed material, [3].

In Figure 4 the indicates VZ mean voids, CB carbon fibre cables and AR are areas with resin saturated. Before the test specimens were performed micrography analysis to obtain quality of manufacture. This point is very important to identify some common problems that can influence results of test. In a second point of this micrography, after the test, some parts of specimens are cut in specific positions and evaluate the characteristics of fracture.

3.1 Micrography preparation of sample manufacture

The objective of micrograph analysis on this section is evaluate the manufacturing properties, in specific the porosity level and voids on manufactured part. The analysis are accomplished on manufacture specimen but not tested. To perform the micrography test of level of porosity and voids it's necessary to cut some specimens in different positions of manufactured specimen, as show in figure 5. Were cut eight samples with dimension of 6 x 6 x 12 mm, as identified on the specimen.

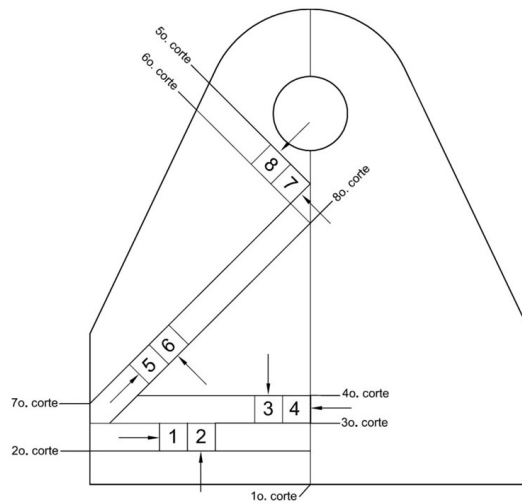


Figure 5 – Sample cutting scheme of manufactured specimen for analysis level of porosity and voids.

In figure 6 as show the sequence to obtain samples cut from untested specimen to evaluate quality of manufacture in terms of voids and porosity.

3.2 Micrography preparation of sample fracture region

The main objective of micrograph analysis on this section is to evaluate the fracture characteristics in the micro-structure of the material after tested specimen, more specifically to seek and identify the type of fracture that occurred in the catastrophic failure of the specimen region. To carry out the



Figure 6 – Cut and preparation samples for analysis level of porosity and voids.

micrograph analysis, verifying the type of failure that occurred after the specimen tests, it is necessary to cut several samples at pre-defined sampling positions, as shown in figure 7.

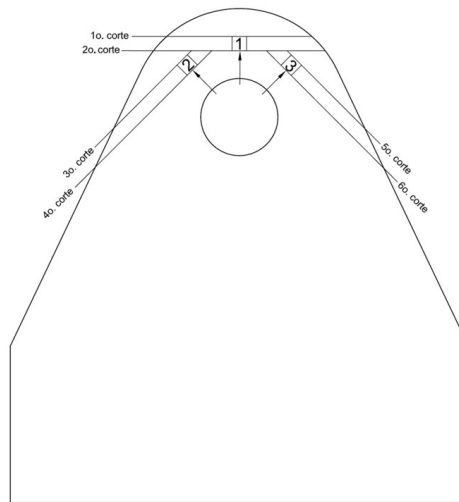


Figure 7 – Sample cutting scheme of manufactured specimen for analysis of characteristics of fracture.

In particular, the samples were taken from the same positions where the strain gauges were attached and positioning of 0° and 45° . In figure 8 as show specimen before the test with strain gauges.



Figure 8 – Specimen with strain gauges attached before the test.

In figure 9 present region failure of specimen after the test and region will be obtained samples of micrographic analysis. Samples were taken only from specimens weren't completely fractured and could not be separated after test, as there were conditions to keep them together after cutting and give analysis condition.



Figure 9 – Specimen with strain gauges attached on fracture region after the test.

4. Characteristics of Numerical Analysis

4.1 Model Failure criteria

The model used to solve the problem is based on the work developed by Donadon *et. al* [4]. To detect damage initiation, the five criteria for all failure modes in the plane are used. They are based

on the maximum stress criterion, according to equations bellow listed in [4]:
Fibre failure in tension

$$F_f^t(\sigma_{11}) = \sigma_{11}/X_t \quad (1)$$

Fibre failure in compression

$$F_f^c(\sigma_{11}) = |\sigma_{11}|/X_c \quad (2)$$

Matrix crack in tension

$$F_m^t(\sigma_{22}) = \sigma_{22}/Y_t \quad (3)$$

Matrix failure in compression

$$F_m^c(\sigma_{22}) = \sigma_{22}/Y_c \quad (4)$$

Plain failure in shear

$$F_m^s(\tau_{12}) = \tau_{12}/S \quad (5)$$

The simbology X_t , X_c , Y_t , and Y_c refer to respectively resistance in tension and compression of fibre and matrix direction. S_{12} is shear resistance in plane.

The interfibre failure mode (IFF) consist in matrix transversal crack for tension or compression, according to Donadon *et. al* [4].

Based on results of work Soden *et. al* [6] and Pinho-a *et. al* [7], and Pinho-b *et. al* [8], the failure envelope based on the transverse stress σ_2 and shear in plane τ_{12} is described by a criteria of quadratic interactions. Thus, the failure development is based on quadratic failure interactions criteria, as used by Pinho-a *et. al* [7], and Pinho-b *et. al* [8], to predict the propagation of the transverse crack in the stress matrix. The crack in the stress matrix based on the quadratic interactive failure criteria and can be written in terms of tensile and shear stress, according to equation 6:

$$F_f^t(\sigma_{22}, \tau_{23}, \tau_{12}) = (\sigma_{22}/Y_t)^2 + (\tau_{23}/S_{23})^2 + (\tau_{12}/S_{12})^2 \quad (6)$$

Where S_{23} is the shear strength along the thickness.

4.2 Damage evolution

The crack propagation formulation can be used to define the damage evolution process in each failure mode. Internal variables of damage can be used to degrade the stresses associated with each failure mode. Internal variables relate a specific volume or volumetric energy to the material's strain release rate through the characteristic length l^* . The characteristic length l^* is used to map the size of the process zone within the finite element domain, according to Donadon *et. al* [4].

4.2.1 Evolution of damage to fibre failure

The fibre failure criteria is defined by equations 1 and 2. The evolution of damage proposed to fibre failure according to Donadon *et. al* [4] is given by:

$$d_{11}(\lambda_1^f, \lambda_2^f) = \lambda_1^f + \lambda_2^f + \lambda_1^f \lambda_2^f \quad (7)$$

4.2.2 Evolution of damage to matrix failure

The matrix failure criteria is defined by equations 3 and 4. The evolution of damage proposed to matrix failure according to Donadon *et. al* [4] is given by:

$$d_{22}(\lambda_1^m, \lambda_2^m) = \lambda_1^m + \lambda_2^m + \lambda_1^m \lambda_2^m \quad (8)$$

4.2.3 Evolution of damage to in-plane shear failure

The shear-in plane failure criteria is defined by equation 5. The evolution of damage proposed to shear-in plane failure according to Donadon *et. al* [4] is given by:

$$d_{12}(\gamma_{12}) = \gamma_{12f}(2(\gamma_{12} - \gamma_{12,0}^i) - \gamma_{12f}) / (\gamma_{12f} + \gamma_{12,0}^i - \gamma_{12})(\gamma_{12} - \gamma_{12,0}^i) \quad (9)$$

More details about equations of evolution of damages fibre, matrix and in-plane shear failures can be found in the work carried out by Donadon *et. al* [4], [5], and Yokoyama *et. al* [9].

4.2.4 Degradation procedure

The proposed relationship between the degradation stress vector $(\sigma)^d$ and the elastic stress vector $(\sigma)^e$ for a plane stress element according to Donadon *et. al* [4] is given by:

$$\begin{pmatrix} \sigma_{11} \\ \sigma_{22} \\ \sigma_{12} \end{pmatrix} = \begin{bmatrix} (1 - d_{11}(\lambda_1^f, \lambda_2^f)) & 0 & 0 \\ 0 & (1 - d_{11}(\lambda_1^f, \lambda_2^f))(1 - d_{22}(\lambda_1^m, \lambda_2^m)) & 0 \\ 0 & 0 & (1 - d_{12}(\gamma_{12})) \end{bmatrix} \begin{Bmatrix} \sigma_{11} \\ \sigma_{22} \\ \sigma_{12} \end{Bmatrix}^e \quad (10)$$

The proposed orthotropic relationship between the degraded stress and the intact stress is given by equation 10, ensuring that the stiffness matrix is positive and defined during the degradation process.

4.2.5 FEM model - Non-linear hybrid (2D and 3D) modeling to determine the catastrophic failure

A hybrid model was developed that includes a transition between 2D and 3D geometry, simulating a more real test condition. After ensuring the location of the catastrophic failure in the test specimen, it was possible to create a model with this transition between 2D and 3D idealizing the problem, since the analysis area of the catastrophic failure of the specimen is limited only to the part of the upper hole; therefore, it is not necessary to model all 3D geometry. Also taking into account that the processing time and problem solving would increase considerably if the model were completely modeled in 3D. The details of the hybrid model are described in figure 10.

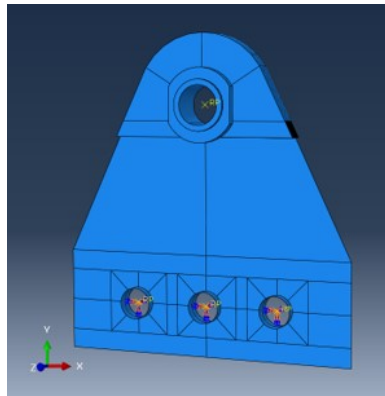


Figure 10 – All parts of the numeric model.

On the lower part of the numerical model three screws are mounted in the three holes at the bottom of the specimen, and the three translations and three rotations of each screw were restricted according to the reference coordinate system, simulating the assembly of test specimen and simulating condition on numeric model.

The lower part of the numeric model was made with 3D deformable shell-like elements, and the geometry is illustrated in figure 11.

The upper part of the model was made with 3D deformable shell-like elements, but with characteristics and mechanical properties along the thickness, defining the number of layers of the model. A sleeve was inserted into the hole in the upper part of the specimen. Rotation on all axes and displacement on the axis perpendicular to the load application (z axis) were restricted for this element. On the inside of the sleeve, a prescribed displacement δ was applied in the y direction of 2 mm, simulating the test condition. The contact condition between the sleeve modeled as 3D deformable and

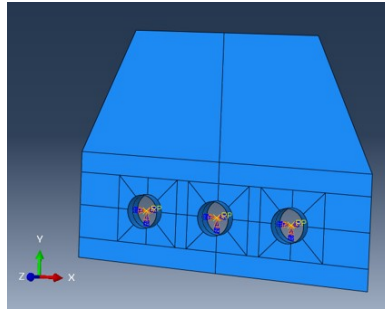


Figure 11 – The lower part of the numeric model.

the lug was characterized. On the numerical model was used element C3D8R with the mechanical properties of the material. The element used for modeling the CDP is called S4R, a classic element for modeling laminated surfaces in composite materials in ABAQUS/Explicit. The element has four nodes and reduced integration.

The upper part of the numeric model is illustrated in figure 12.

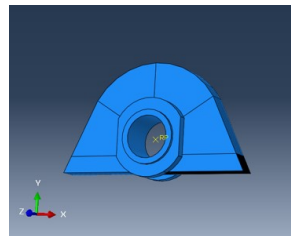


Figure 12 – The upper part of the numeric model.

These layers are modelling of the upper and lower parts as follows:

$$[+45, -45, 0, 90, 90, 0, -45, +45]_{6T}$$

At the interface of the two parts, a transition region was modeled between the solid part and the shell part of the model, allowing the transfer of efforts between the sub-components, in a way that does not affect the results. Figure 13 represents the hybrid model with the mesh and boundary conditions.

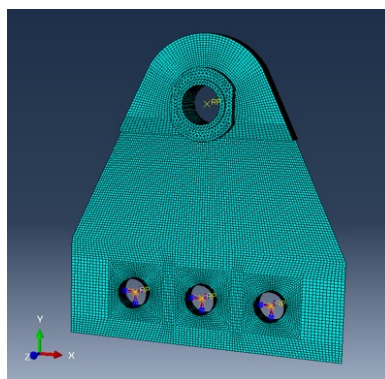


Figure 13 – Hybrid numerical model (2D and 3D) with the mesh and boundary conditions.

The model simulated the non-linear condition according to the “Model Failure Criteria”, using the failure model mentioned in the item “Damage evolution”, implemented in the Fortran software.

With this analysis, the catastrophic failure of the finite element model was evaluated, using the hybrid model to compare the numerical results with the experimental results. The results will be present on next sections.

5. Results

5.1 Results of test specimen analysis

5.1.1 Analysis of the micro-structural integrity of the specimen

From the manufacturing point of view, some samples were analysed in order to characterize possible macro-damage in the micro-structure of the material. In figure 14 presents a typical image of the micro-structure of the material with fibre orientation and resin matrix.

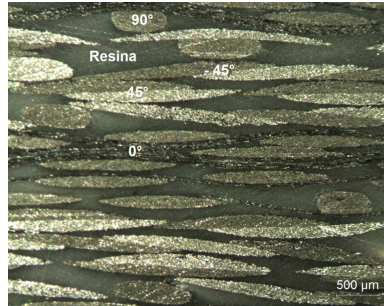


Figure 14 – Photomicrographs section of analysed material, [3].

From the images obtained of the micro-structure of the material, no macro-defects are identified that could compromise the structural integrity of the specimen.

5.1.2 Results of porosity and voids analysis

In general, it is observed that the voids tend to be located between the ply layers and, preferably, in regions close to areas rich in resin. In general, the voids are located in the resin-rich regions and between the fibres, are small (7-30 μm), and occur infrequently in the analysed samples. The results can be seen in figure 15.

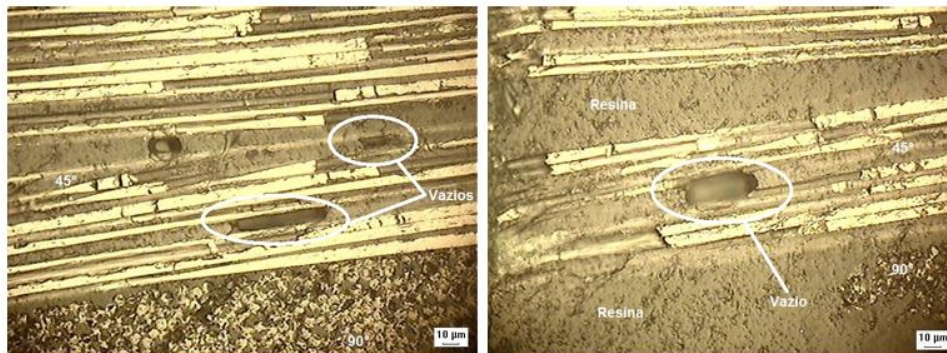


Figure 15 – Micro-voids identified on samples obtained of specimens, 500x magnification.

The identification of porosities in the samples occurs more frequently than the voids. Formation is typically observed in regions rich in resin and with circular and non-circular shapes. Porosities are identified between fibres and in resin-only regions. All occurrences show the formation of micro-porosities (7-30 μm).

Figure 16 show the occurrence of porosities in different samples.

Therefore, the analyses in different positions according to the samples do not show a high occurrence of porosity and voids in the manufactured part and don't affecting the structural integrity of the specimen.

5.1.3 Micrography result analysis of sample fracture region

According to the results obtained, were observed in three samples tested the evidences of the occurrence of many types of failure will be detailed bellow. It is important to observe the positions where the samples were taken from the test specimen described on figure 7.

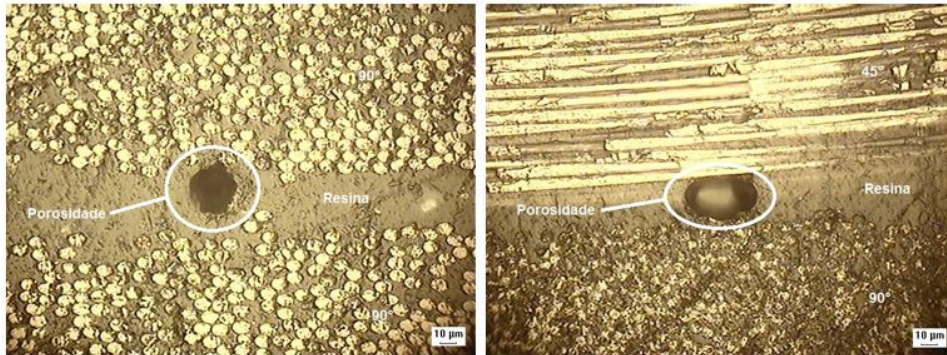


Figure 16 – Micro-porosities identified on sample obtained of specimens, 500x magnification.

It is observed in the specimen 01, position 01 and 02 the evidences of the occurrence of fibre failure by compression and matrix failure by tension . Figures 17 and 18 represents the images obtained at 100x (left) and 200x (right) magnification.

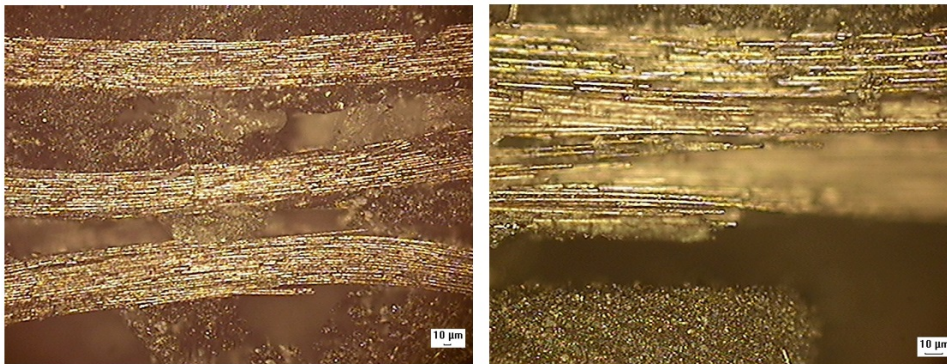


Figure 17 – Fibre failure in compression and matrix failure in tension - position 01.

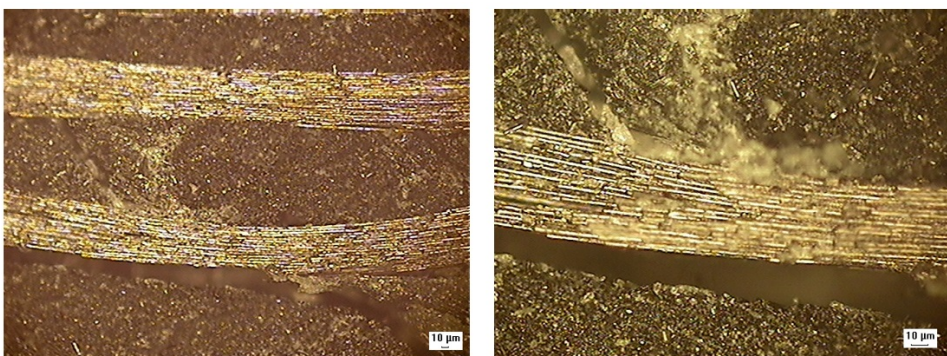


Figure 18 – Fibre failure in compression and matrix failure in tension - position 02.

On the specimen 03 position 01 were observed two types of failure: fibre failure and matrix failure by tension. The results are show in figures 19 represents the images obtained at 100x (left) and 200x (right) magnification.

In the same specimen on position 02 was observed two types of failure: matrix by tension and fibre by compression as show in figure 20:

For specimen 04 in the position 01 was identified fibre failure by compression and matrix failure by tension as show in figure 21. On position 02 is evidenced only fibre failure by tension according to 22.

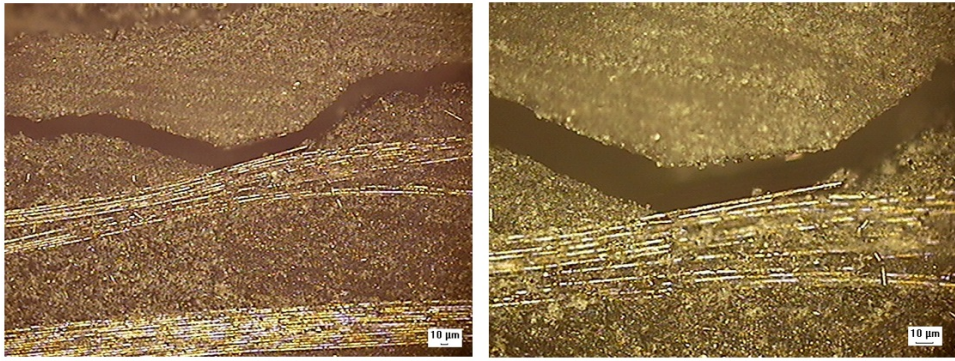


Figure 19 – Fibre failure and matrix failure by tension - position 01.

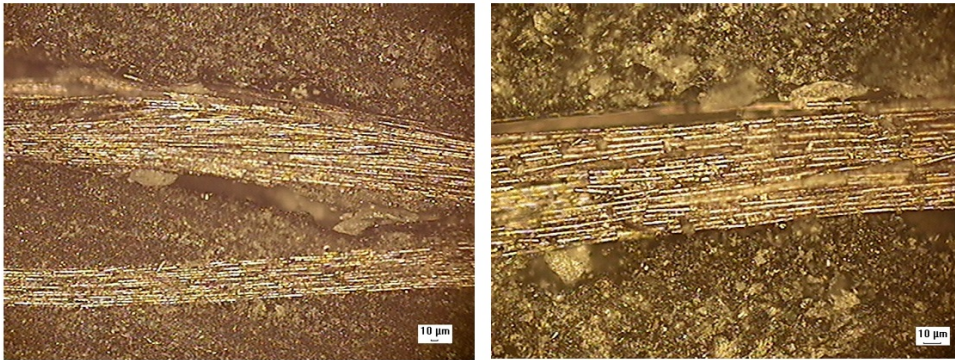


Figure 20 – Fibre failure in compression and matrix failure in tension - position 02.

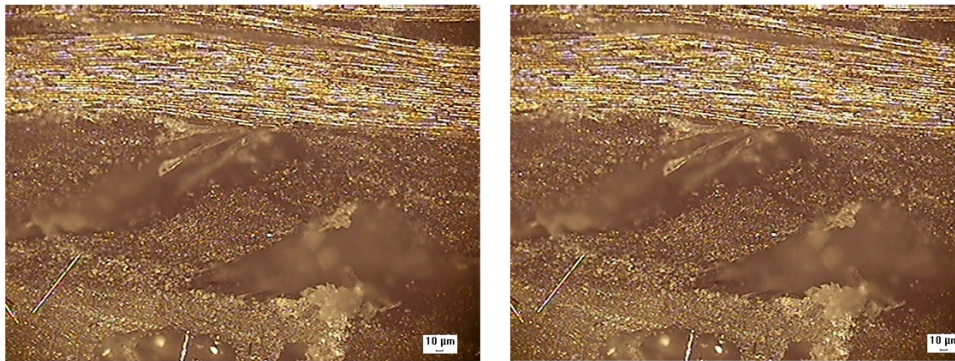


Figure 21 – Fibre failure in compression and matrix failure in tension - position 01.

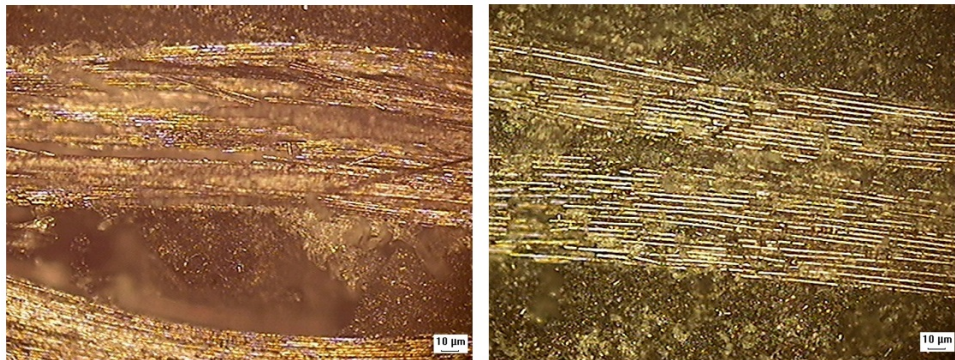


Figure 22 – Fibre failure in tension - position 02.

5.2 Results of numerical model analysis

The results of load as a function of displacement obtained from the proposed hybrid numerical model (2D and 3D) is shown in figure 23, where the behavior of the lug up to catastrophic failure is repre-

sented.

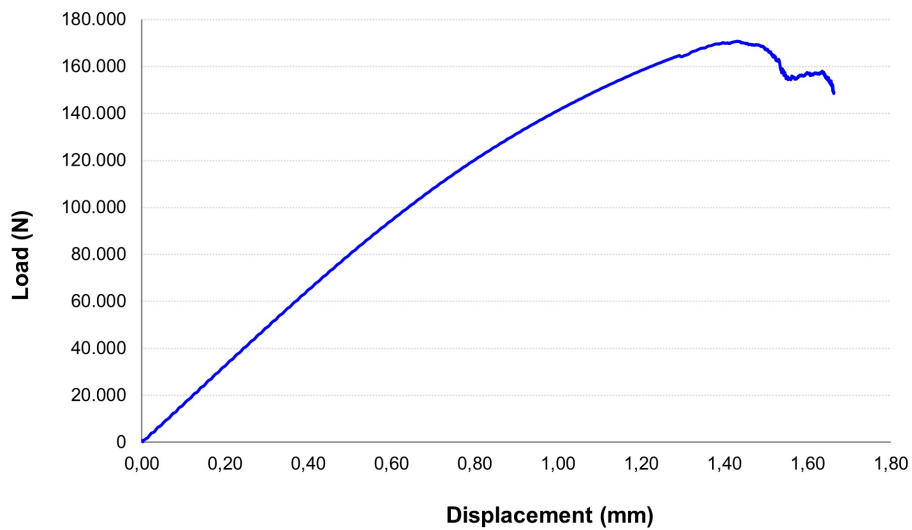


Figure 23 – Load versus displacement obtained from the hybrid numerical model (2D and 3D).

5.2.1 Failure modes of the hybrid numerical model (2D and 3D)

All failure modes obtained in the finite element models are detailed and presented in the following Figures.

For the tension fibre failure mode, the finite element model presents the behavior as described on figure 24 and shows a detail of the internal region of the hole.

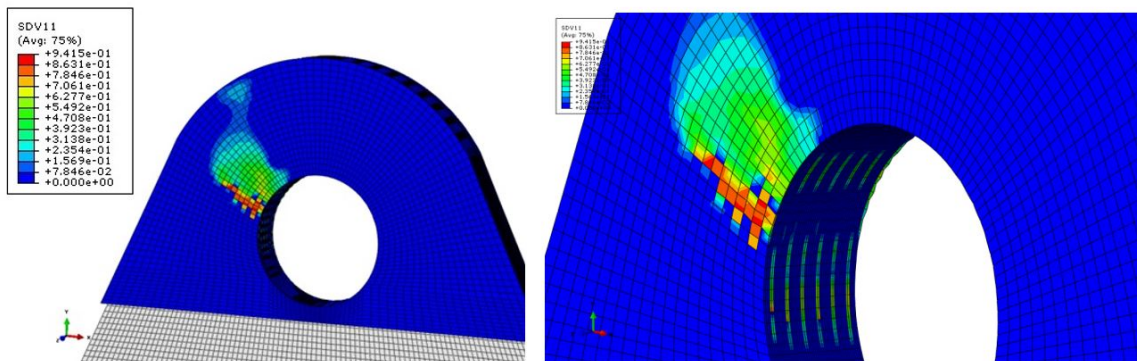


Figure 24 – Tension fibre failure mode - position 02.

For the compression fibre failure mode, the finite element model presents the behavior as described on figure 25 and shows a detail of the internal region of the hole.

For the tension matrix failure mode, the finite element model presents the behavior as described on figure 26 and shows a detail of the internal region of the hole.

For the shear matrix failure mode, the finite element model presents the behavior as described on figure 27 and shows a detail of the internal region of the hole.

The compression failure in the matrix was evaluated in the finite element model, but it is not significant to the point of presenting damage to the model. The same is true for inter-fibre failure, including transverse compression failure.

5.3 Comparative analysis of experimental and numerical results

The comparative results described below will be compare results based on finite element model comparing the test results of the specimen. All the results (test specimen and finite element model)

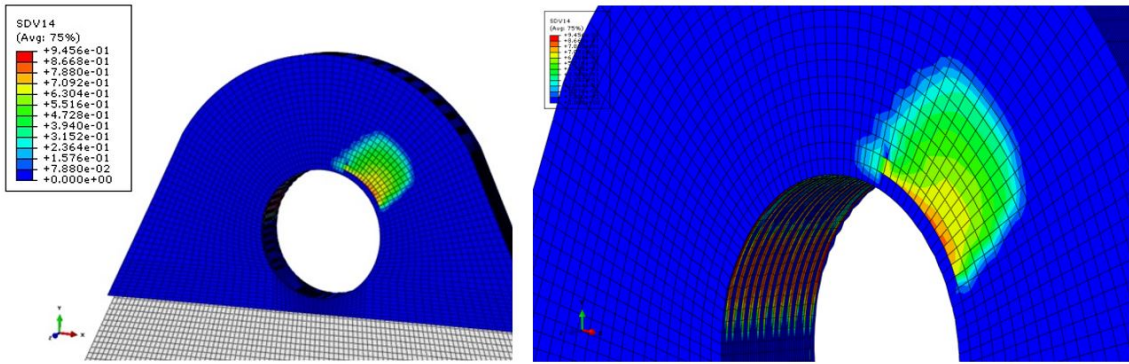


Figure 25 – Compression fibre failure mode - position 01 and 03.

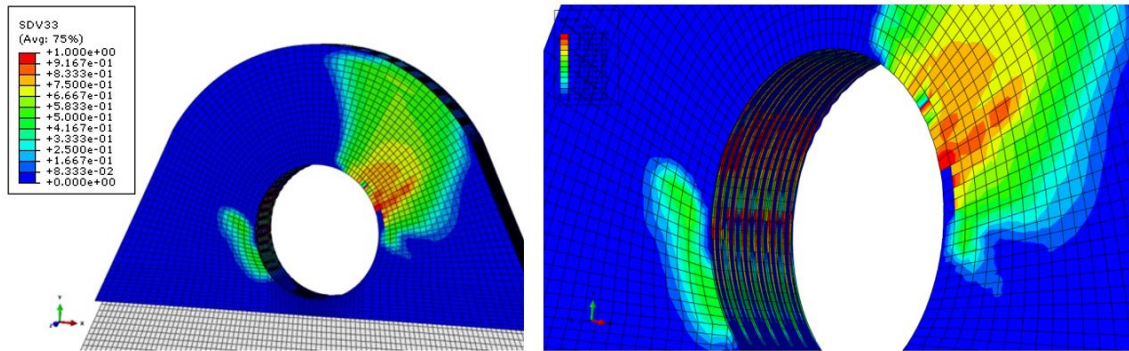


Figure 26 – Tension matrix failure mode position 01 and 3.

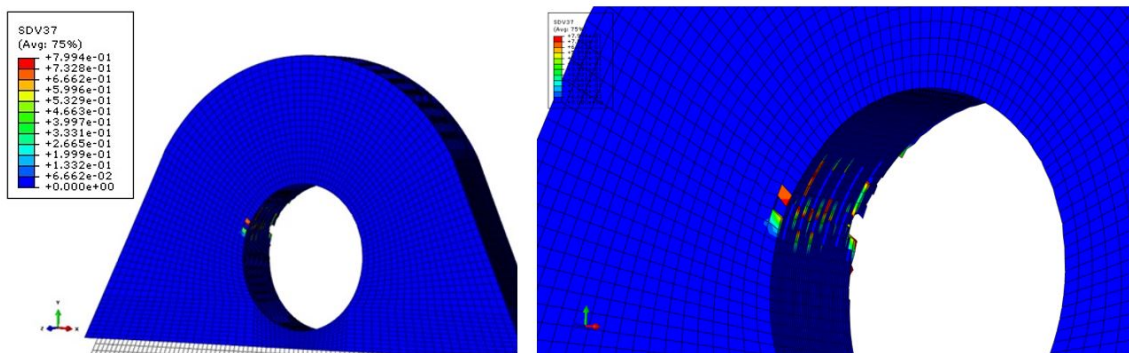


Figure 27 – Shear matrix failure mode - position 02.

are based on the positions described in figure 7.

Across region 1, the failure modes results were obtained in the fibre by compression and matrix by tension. The correlation between the results obtained from figure 17 of the experimental results from numerical results as show on figure 25 (fibre compression), and figure 26 (matrix tension).

Across region 2, the failure modes results were obtained in the fibre by tension and matrix by tension and shear. The correlation between the results obtained from figure 18 of the experimental results from numerical results as show on figure 24 (fibre tension), figure 26 (matrix tension), and figure 27 (matrix shear).

6. Conclusions

The hybrid model (2D and 3D) is able to represent the behavior of the lug made of composite material subjected to tension loading, obtaining the value of the failure load and its failure modes, comparing the numerical results with the results obtained in the experimental tests.

The failure routine used in the hybrid model (2D and 3D) demonstrates robustness according to

the proposed objective, since the numerical model results refer to failures very close to the results obtained in the experimental tests.

Given the results, a more detailed analysis of the fracture in the micrographic area is also necessary, such as the use of tomography or other technology to obtain more information.

7. Copyright Statement

The authors confirm that they, and/or their company or organization, hold copyright on all of the original material included in this paper. The authors also confirm that they have obtained permission, from the copyright holder of any third party material included in this paper, to publish it as part of their paper. The authors confirm that they give permission, or have obtained permission from the copyright holder of this paper, for the publication and distribution of this paper as part of the ICAS proceedings or as individual off-prints from the proceedings.

8. Contact Author Email Address

giovane.fonseca@embraer.com.br

giovane@ufmg.br

References

- [1] Knight JR. N.F. Reeder J.R. Ransom J.B., Glaessgen E.H. Raju I.S. Lessons learned from recent failure and incident investigations of composite structures. *49th AIAA/ASME/ASCE/AHS/ASC Structures, Structural Dynamics, and Materials*, 2008.
- [2] Jevons M. Vali-Shariatpanahi S. Evaluation of failure in pin-loaded laminates. *49th AIAA/ASME/ASCE/AHS/ASC Structures, Structural Dynamics, and Materials*, 2008.
- [3] Ancelotti Junior A. C. Efeitos da Porosidade na Resistência ao Cisalhamento e nas Propriedades Dinâmicas de Compósitos de Fibra de Carbono/Resina Epóxi. *Tese de Mestrado – Instituto Tecnológico de Aeronáutica, Curso de Pós-Graduação em Engenharia Mecânica e Aeronáutica, Área de Física e Química dos Materiais Aeroespaciais*, 2006.
- [4] Donadon M. V. Almeida S. F. M. Faria A. R. Arbelo M. A. A Three-Dimensional Ply Failure Model for Composite Structures. *International Journal of Aerospace Engineering*, p. 22, Article ID 486063, doi: 10.1155/2009/486063., 2009.
- [5] Donadon M. V. Almeida S. F. M. Faria A. R. Arbelo M. A. An energy based failure model for FRP laminates. *Composite Structures*, v. 93, pp. 143-152, 2010.
- [6] Soden P. Hinton M. J. Kaddour A. S. Biaxial test results for strength and deformation of a range of E-glass and carbon fiber reinforced composite laminates: failure exercise benchmark data. *Composites Science and Technology*, v. 62, no. 12-13, pp. 1489–1514, 2002.
- [7] Pinho S. Iannucci, L. Robinson, P. Physically-based failure models and criteria for laminated fiber reinforced composites with emphasis on fiber kinking—part I: development. *Composites: Part A*, v. 37, no. 1, pp. 63–73, 2006a.
- [8] Pinho S. Iannucci, L. Physically-based failure models and criteria for laminated fiber reinforced composites with emphasis on fiber kinking: part II: FE implementation. *Composites: Part A*, v. 37, no. 5, pp. 766–777, 2006b.
- [9] Yokoyama N. O. Donadon, M. V. Almeida, S. F. M. A numerical study on the impact resistance of composite shells using an energy based failure model. *Composite Structures*, v. 93, p. 142-152, 2010.